

Research Article

Preparation and Characterization of PEG4000 Palmitate/PEG8000 Palmitate-Solid Dispersion Containing the Poorly Water-Soluble Drug Andrographolide

Qingyun Zeng, Liquan Ou, Guowei Zhao , Ping Cai, Zhenggen Liao, Wei Dong, and Xinli Liang

Key Laboratory of Modern Preparation of Traditional Chinese Medicine, Ministry of Education, Jiangxi University of Traditional Chinese Medicine, Nanchang 330004, China

Correspondence should be addressed to Guowei Zhao; weiweihaoyunqi@163.com

Received 4 December 2019; Revised 21 January 2020; Accepted 20 February 2020; Published 19 March 2020

Guest Editor: Yu Tao

Copyright © 2020 Qingyun Zeng et al. This is an open access article distributed under the Creative Commons Attribution License, which permits unrestricted use, distribution, and reproduction in any medium, provided the original work is properly cited.

Solid dispersion (SD) is the effective approach to improve the dissolution rate and bioavailability of class II drugs with low water solubility and high tissue permeability in the Biopharmaceutics Classification System. This study investigated the effects of polyethylene glycol (PEG) molecular weight in carrier material PEG palmitate on the properties of andrographolide (AG)-SD. We prepared SDs containing the poorly water-soluble drug AG by the freeze-drying method. The SDs were manufactured from two different polymers, PEG4000 palmitate and PEG8000 palmitate. The physicochemical properties of the AG-SDs were characterized by Fourier transform infrared spectroscopy, thermogravimetric analysis, differential scanning calorimetry, powder X-ray diffraction, scanning electron microscopy, dissolution testing, and so on. We found that AG-PEG4000 palmitate-SD and AG-PEG8000 palmitate-SD were similar in the surface morphology, specific surface area, and pore volume. Compared with the AG-PEG4000 palmitate-SD, the intermolecular interaction between PEG8000 palmitate and AG was stronger, and the thermal stability of AG-PEG8000 palmitate-SD was better. In the meanwhile, the AG relative crystallinity was lower and the AG dissolution rate was faster in AG-PEG8000 palmitate-SD. The results demonstrate that the increasing PEG molecular weight in the PEG palmitate can improve the compatibility between the poorly water-soluble drug and carrier material, which is beneficial to improve the SD thermal stability and increases the dissolution rate of poorly water-soluble drug in the SD.

1. Introduction

Oral administration is the most common route of administration due to its convenience, low cost, and flexible design. However, a major disadvantage of oral administration is the low bioavailability, usually due to poor water solubility and low permeability of active pharmaceutical ingredients (API) [1].

Although Class II drugs in the Biopharmaceutics Classification System (BCS) have high tissue permeability, their oral bioavailability is commonly low. This means that bioavailability is solubility dependent [1]. Therefore, one of the major challenges of the pharmaceutical industry is to apply strategies which can improve the solubility of these drugs to

develop such problematic APIs into orally bioavailable and therapeutic effective drugs [2, 3]. Solid dispersion (SD) is one of the most effective approaches to improve the solubility, dissolution rate, and the bioavailability of poorly water-soluble drugs [4–7]. SD has a wide range of advantages, such as reducing particle size to the molecular level, preventing the agglomeration of the drug particles by the interactions between the drug and carrier material, and releasing drug at supersaturated state, which can improve drug absorption.

Polyethylene glycol (PEG) has a very low melting point and is easily soluble in water and organic solvents. Therefore, PEG is suitable for the preparation of SD by the melting method and the solvent method [8, 9], and it is one of the most commonly used carrier materials in SD. However, PEG

is a hydrophilic polymer and most of Class II drugs are hydrophobic compounds, so the solubility of most drugs in PEG is very limited. The hydrophobic drug in SD is often in a supersaturated state and has a tendency to recrystallize in the preparation process (cooling or solvent removal) and during storage of SD [10–13]. Therefore, in the previous research [14], the carbon chain was grafted on PEG to increase the lipophilicity of the hydrophilic carrier material, and the effect of the carrier material lipophilicity on the physico-chemical properties and dissolution behavior of SD was studied. The results showed that in the andrographolide (AG)-SD prepared by PEG-saturated fatty acid ester with different long carbon chains as a carrier material, the crystallinity and the melting temperature reduced and the dissolution rate of AG increased with the increase of the length of carbon chain of PEG-saturated fatty acid ester. This indicated that the increase of carrier material lipophilicity is beneficial to the thermal stability of SD, the decrease of crystallinity, and the increase of dissolution rate of poorly water-soluble drug in the SD.

Andrographolide (AG), a diterpenoid lactone, is isolated from the Chinese herb *Andrographis paniculata*. It has been proved to have many pharmacological actions, such as analgesic, antipyretic, anti-inflammatory, antiviral, and anticancer [15–18]. The potential use of AG has attracted great attention in recent years. AG has low aqueous solubility (74 $\mu\text{g}/\text{ml}$). The therapeutic use of AG is restricted by its poor solubility in water, which results in low bioavailability after oral administration. Therefore, AG was still chosen as a model drug to further study the effect of PEG molecular weight on the SD properties when PEG fatty acid was used as the carrier material for preparing SD.

2. Materials and Methods

2.1. Materials. Andrographolide (AG) was purchased from Hao-Xuan Biotechnology Co., Ltd. (Xi'an, China). The PEG4000 palmitate and PEG8000 palmitate were synthesized in the laboratory.

2.2. Preparation of Physical Mixture (PM). The physical mixtures of AG and the carrier material with a batch size of 3 g were prepared by mixing the components with a pestle in a mortar and using geometric dilution. The mixtures were sieved using a mesh of 250 μm . The drug: carrier weight ratio was 1:3 (w/w) [14]. The samples were labeled as AG-PEG4000 palmitate-PM and AG-PEG8000 palmitate-PM, respectively. The samples were stored in a desiccator over silica gel prior to use to decrease the potential effect of hygroscopicity.

2.3. Preparation of AG-SD by Freeze-Drying Method. The PM was dissolved in 30% ethanol using a magnetic stirrer. The solution was frozen at liquid nitrogen for 1 h and subsequently freeze-dried for 24 h at -40°C using a FreeZone freeze-dryer (Labconco Corp., USA). The powder was collected and then stored in a desiccator over silica gel prior to use to decrease the potential effect of hygroscopicity. The

prepared SDs were labeled as AG-PEG4000 palmitate-SD and AG-PEG8000 palmitate-SD, respectively.

2.4. Fourier Transform Infrared Spectroscopy (FT-IR). A Spectrum Two FT-IR spectrometer (PerkinElmer Corp., USA) was used for collecting the spectra. A small amount of each sample was placed in a mortar with potassium bromide and triturated with a pestle, which was compressed into a disc by using a FW-4A powder compressing instrument (Uncommon Sci. Tech. Development Co., Ltd., Tianjin, China). The spectral region from 400 to 4000 cm^{-1} was collected as an accumulation of 64 scans.

2.5. Thermogravimetric (TG) Analysis. TG analysis of SDs and physical mixtures was determined by a TG/DTA6300 thermal analysis instrument (SII Nano Technology Inc., Japan). The samples ($\sim 5\text{ mg}$) were placed in open aluminum pans and heated from 30°C to 500°C at $10^\circ\text{C}/\text{min}$.

2.6. Powder X-Ray Diffraction (XRD). XRD analysis of samples was conducted by using an X-ray diffractometer (D8 Advance, Bruker) with a copper anode ($\text{Cu K}\alpha$ radiation). The operating voltage and current were set to 40 kV and 40 mA, respectively. The diffraction pattern was measured at room temperature with 2θ scanning from 5° to 55° .

2.7. Differential Scanning Calorimetry (DSC). The samples ($\sim 5\text{ mg}$) were placed in standard aluminum pans and sealed. The crimped pans were heated from 20°C to 270°C at a scanning rate of $10^\circ\text{C}/\text{min}$ using nitrogen gas (20 mL/min) to purge the DSC. A Diamond DSC instrument (PerkinElmer Corp., USA) was calibrated using pure indium before measurement.

2.8. Scanning Electron Microscopy (SEM). A Quanta 250 scanning electron microscope (FEI Corp., USA) was used to generate electron micrograph images. The SDs and physical mixtures were mounted on an aluminum stub using double-sided adhesive tape. The samples were then sputter-coated with gold for 60 s. Micrographs with different magnifications were taken to determine the surface morphology of SDs and physical mixtures.

2.9. Specific Surface Area and Pore Volume. The surface area and pore volume of different grades of SDs and physical mixtures were determined by nitrogen adsorption technique using a TriStar3000 surface area and pore volume analyzer (Micromeritics Instrument Corp., USA) [19, 20]. Moisture was removed from the samples prior to the surface area measurement by nitrogen flow at room temperature overnight using a Flow Pre-degasser (Micromeritics Instrument Corp., USA).

2.10. High-Performance Liquid Chromatography (HPLC) Analysis. An Agilent 1260 HPLC system (Agilent Corp.,

USA) with a C_{18} column (150 mm \times 4.6 mm, 5 μ m) was used for the AG analysis. A mobile phase of methanol and water (60:40, V: V) was used at a flow rate of 1 mL/min. A UV detector was utilized, and the absorption peak for AG was investigated at a maximum wavelength of 225 nm.

2.11. Dissolution Testing. The drug release was performed using the Chinese Pharmacopoeia paddle method with a ZRS-8G dissolution tester (Tianda Tianfa Technology Co., Ltd., China). The 900 mL redistilled water in the dissolution vessels was heated and maintained at $37 \pm 0.5^\circ\text{C}$. The samples (0.10 g) were placed into the dissolution vessels at a rotation rate of 100 rpm. The 1.5 mL aliquots were withdrawn at predetermined time intervals (5, 10, 15, 30, 45, 60, 90, and 120 min) and filtered with a 0.22 μ m membrane filter. An equal volume of fresh medium was added to keep an invariable dissolution volume in the meantime. The obtained filtrates were analyzed according to the aforementioned HPLC condition.

2.12. Statistical Analysis. The cluster analysis was calculated using SPSS19.0 software.

3. Results and Discussion

3.1. FT-IR. Figure 1 shows the FT-IR spectra of pure AG, physical mixtures, and SDs. The $-\text{OH}$ absorption peak in pure AG is at 3317 cm^{-1} , the absorption peak position was not shifted or shifted slightly in all the physical mixtures, and the absorption peak position in the AG-PEG4000 palmitate-SD and the AG-PEG8000 palmitate-SD was blue shifted to 3326 cm^{-1} and 3339 cm^{-1} , respectively. This indicated that there was an intermolecular interaction between AG and PEG palmitate after the preparation of SD, which may form a hydrogen bond. The intermolecular hydrogen bonds between the drug and the carrier material facilitated the stability of the SD during storage [21, 22]. Moreover, compared with AG-PEG4000 palmitate-SD, the blue shift of the $-\text{OH}$ absorption peak in AG-PEG8000 palmitate-SD was greater. This may be due to the increase of the PEG molecular weight in PEG palmitate, which can increase the lipophilicity of the carrier material, and thus improve the compatibility of PEG palmitate with the poorly water-soluble drug AG.

3.2. TG. The TG analysis of pure AG, physical mixtures, and SDs is shown in Figure 2. The 5% weight-loss temperature (T_i) of all samples is listed in Table 1. As can be seen from Table 1, the T_i of the prepared SDs and physical mixtures was significantly higher than that of pure AG. The T_i of the SD was 1°C – 3°C higher than the corresponding physical mixture. This indicated that the interaction between AG and the carrier material in the SD was greater than the physical mixture. This was due to the fact that AG and carrier materials are in contact with each other in the molecular form in the preparation process of SD, which is more advantageous to enhance the intermolecular interaction than the preparation process of physical mixtures.

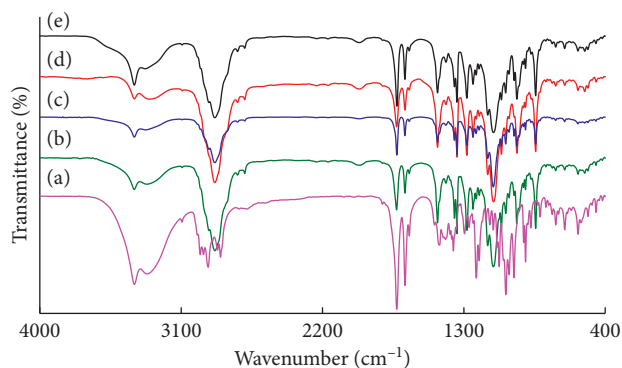


FIGURE 1: FT-IR spectra of (a) pure AG, (b) AG-PEG4000 palmitate-PM, (c) AG-PEG4000 palmitate-SD, (d) AG-PEG8000 palmitate-PM, and (e) AG-PEG8000 palmitate-SD.

The T_i of the physical mixture and SD prepared with PEG8000 palmitate as a carrier material was significantly increased as compared to the physical mixture and SD prepared with PEG4000 palmitate as a carrier material. This may be due to the higher compatibility of PEG8000 palmitate with poorly water-soluble drug AG, thereby increasing the thermal stability of the SD and physical mixture prepared with PEG8000 palmitate as the carrier material.

3.3. XRD. To confirm the crystalline structure of AG and the effect of carriers on it, XRD patterns of pure AG, SDs, and physical mixtures were studied, which are shown in Figure 3. The intense diffraction peaks were observed at 9.78, 11.97, 14.78, 15.67, 17.67, 18.44, and 22.62 2θ degrees, which revealed high crystallinity of AG. Both the SDs and physical mixtures showed the overlap of XRD patterns related to AG. Compared with physical mixtures, the intensity of AG diffraction peaks decreased significantly in the prepared SDs. This indicated that AG was not in the completely crystal state and was in a partial-amorphous and partial-crystal state in the as-prepared SDs.

3.4. DSC. The DSC thermograms of pure AG, physical mixtures, and SDs are shown in Figure 4. Figure 4(a) shows pure AG to have a sharp melting point of 243°C confirming its crystallinity. All the two physical mixtures and two SDs had a strong endothermic peak (T_{m1}) at about 60°C and a weak endothermic peak (T_{m2}) near 210°C – 230°C . The T_{m1} and T_{m2} were the endothermic peaks of PEG palmitate and AG, respectively.

It was observed that the endothermic peak of AG and no glass transition on DSC thermograms of the SDs indicated that AG was not in 100% amorphous state in the SDs. The T_{m2} of SD was about 8°C lower than the corresponding physical mixture (see in Figure 4 and Table 1), which indicated that the existential state of AG in SD was different from that in the corresponding physical mixture. The above results showed that AG existed in partial-crystal and partial-amorphous state in the prepared AG-PEG palmitate-SDs. The result was consistent with that of XRD.

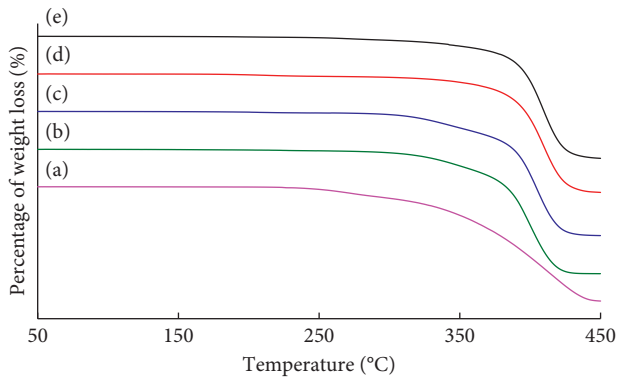


FIGURE 2: TG curves of (a) pure AG, (b) AG-PEG4000 palmitate-PM, (c) AG-PEG4000 palmitate-SD, (d) AG-PEG8000 palmitate-PM, and (e) AG-PEG8000 palmitate-SD.

TABLE 1: T_i and T_m of pure AG, physical mixtures (PM) and SD.

Sample	T_i (°C)	T_{m1} (°C)	T_{m2} (°C)
AG	272		243
AG-PEG4000 palmitate-PM	318	60	228
AG-PEG4000 palmitate-SD	319	57	220
AG-PEG8000 palmitate-PM	323	64	226
AG-PEG8000 palmitate-SD	326	61	218

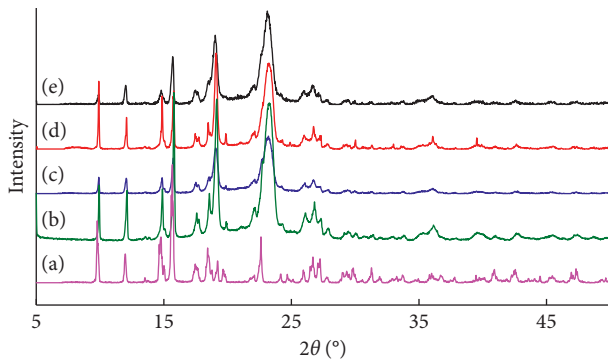


FIGURE 3: XRD patterns of (a) pure AG, (b) AG-PEG4000 palmitate-PM, (c) AG-PEG4000 palmitate-SD, (d) AG-PEG8000 palmitate-PM, and (e) AG-PEG8000 palmitate-SD.

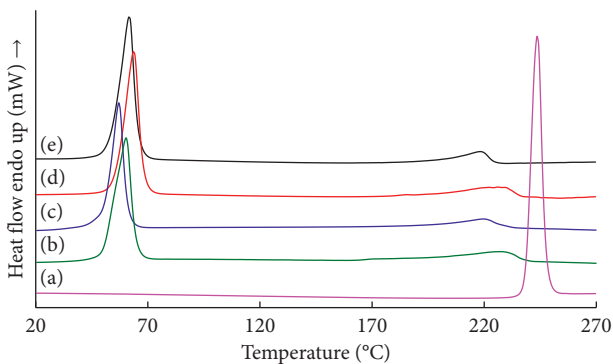


FIGURE 4: DSC thermograms of (a) pure AG, (b) AG-PEG4000 palmitate-PM, (c) AG-PEG4000 palmitate-SD, (d) AG-PEG8000 palmitate-PM, and (e) AG-PEG8000 palmitate-SD.

Table 1 shows that the T_m of AG-PEG8000 palmitate-SD is lower than that of the AG-PEG4000 palmitate-SD, which indicates that increasing the molecular weight of PEG in the carrier material can improve the compatibility of the carrier material with the poorly water-soluble drug AG. Therefore, the relative crystallinity of AG in SD prepared by PEG8000 palmitate was decreased.

3.5. SEM. In order to determine the surface morphology of SDs, SEM analysis of the samples was performed. As shown in Figure 5, pure AG was a smooth block-shaped crystal, the physical mixtures were an irregular block-shaped particle with a rough surface, and SD showed sheet-like particles.

3.6. Specific Surface Area and Pore Volume. Table 2 shows the specific surface area and pore volume of the physical mixtures and SDs. The specific surface area and pore volume of SDs increased significantly compared to the physical mixtures. This was because the SD powders prepared by the freeze-drying method were loose and showed sheet-like particles; therefore, they had a larger specific surface area and pore volume.

3.7. Dissolution Testing. The dissolution of a poorly water-soluble drug is crucial where it is the rate-limiting step in the oral absorption process from a solid dosage form and is an important parameter related to bioavailability [23–25]. Results of dissolution testing for pure AG, physical mixtures, and SDs are presented in Figure 6. The physical mixtures displayed dissolution profiles superior to that of pure AG, whereas the SDs displayed dissolution profiles superior to that of pure AG and the physical mixtures.

In order to further study the effect of carrier material on the dissolution behavior of AG in the SDs, the difference factor (f_1) [26] was used to compare the dissolution curves of AG in AG-PEG8000 palmitate-SD and AG-PEG4000 palmitate-SD. An f_1 value between 0 and 15 indicates that the dissolution behavior of the experimental formulation is similar to that of the reference formulation. The f_1 is calculated according to the following equation:

$$f_1 = \frac{\sum_{t=1}^n |R_t - T_t|}{\sum_{t=1}^n R_t}, \quad (1)$$

where R_t was the dissolution rate of reference formulation (AG-PEG4000 palmitate-SD) at different time points and T_t was the dissolution rate of experimental formulation (AG-PEG8000 palmitate-SD) at different time points. The f_1 value of AG-PEG8000 palmitate-SD versus AG-PEG4000 palmitate-SD was calculated to be 41. The results showed that increasing the molecular weight of PEG could improve the compatibility of the carrier material with the poorly water-soluble drug AG, thus promoting the dissolution of AG from SD.

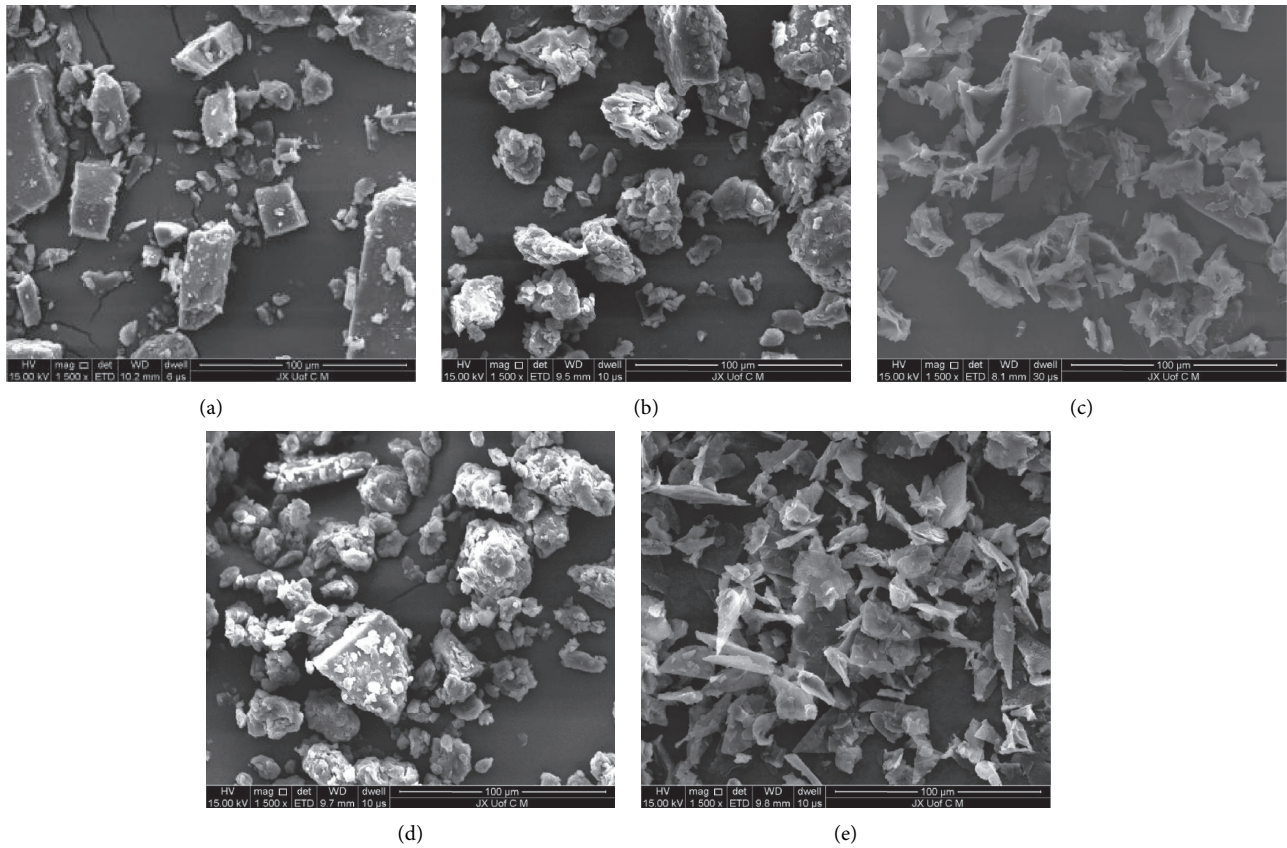


FIGURE 5: SEM photographs of (a) pure AG, (b) AG-PEG4000 palmitate-PM, (c) AG-PEG4000 palmitate-SD, (d) AG-PEG8000 palmitate-PM, and (e) AG-PEG8000 palmitate-SD.

TABLE 2: Specific surface area and pore volume of physical mixtures (PM) and SDs.

Sample	Specific surface area (m ² /g)	Pore volume (×10 ⁻³ , m ³ /g)
AG-PEG4000 palmitate-PM	0.4084	1.784
AG-PEG4000 palmitate-SD	1.7350	7.155
AG-PEG8000 palmitate-PM	0.3340	2.694
AG-PEG8000 palmitate-SD	2.5646	5.376

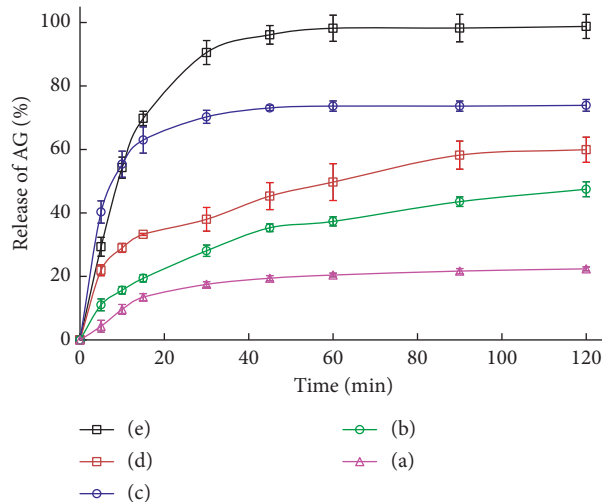


FIGURE 6: Dissolution profiles of (a) pure AG, (b) AG-PEG4000 palmitate-PM, (c) AG-PEG4000 palmitate-SD, (d) AG-PEG8000 palmitate-PM, and (e) AG-PEG8000 palmitate-SD. The error bars represent the standard deviation of measurements in six separate samples ($n = 6$).

4. Conclusions

In this work, the effects of the PEG molecular weight in carrier material PEG palmitate on the properties of AG-SD were investigated. AG-PEG4000 palmitate-SD and AG-PEG8000 palmitate-SD are similar in surface morphology, specific surface area, and pore volume. Compared with the SD with PEG4000 palmitate as a carrier material, the intermolecular interaction between PEG8000 palmitate and AG was stronger and the thermal stability of AG-PEG8000 palmitate-SD was better. In the meanwhile, the AG relative crystallinity was lower and the AG dissolution rate was faster in AG-PEG8000 palmitate-SD. The results demonstrate that increasing the PEG molecular weight in PEG palmitate could improve the compatibility between the poorly water-soluble drug and carrier material, which is beneficial to improve the SD thermal stability and increases the dissolution rate of poorly water-soluble drug in the SD.

Data Availability

The data used to support the findings of this study are available from the corresponding author upon request.

Conflicts of Interest

The authors declare that there are no conflicts of interest regarding the publication of this paper.

Authors' Contributions

Qingyun Zeng and Liquan Ou contributed equally to this work.

Acknowledgments

This research was supported by the National Natural Science Foundation of China (no. 81560654); the Traditional Chinese medicine Administration of Jiangxi Provincial of China (no. 2019A010); the PhD research start up foundation of Jiangxi University of Traditional Chinese Medicine (2019WBZR001); the First-class Discipline of Traditional Chinese Medicine of Jiangxi University of Traditional Chinese Medicine (no. JXSYLXK-ZHYAO058).

References

- [1] Y. S. R. Krishnaiah, "Pharmaceutical technologies for enhancing oral bioavailability of poorly soluble drugs," *Journal of Bioequivalence and Bioavailability*, vol. 2, no. 2, pp. 28–36, 2010.
- [2] G. Van den Mooter, "The use of amorphous solid dispersions: a formulation strategy to overcome poor solubility and dissolution rate," *Drug Discovery Today: Technologies*, vol. 9, no. 2, pp. e79–e85, 2012.
- [3] Y. Kawabata, K. Wada, M. Nakatani, S. Yamada, and S. Onoue, "Formulation design for poorly water-soluble drugs based on biopharmaceutics classification system: basic approaches and practical applications," *International Journal of Pharmaceutics*, vol. 420, no. 1, pp. 1–10, 2011.
- [4] C. L.-N. Vo, C. Park, and B.-J. Lee, "Current trends and future perspectives of solid dispersions containing poorly water-soluble drugs," *European Journal of Pharmaceutics and Biopharmaceutics*, vol. 85, no. 3, pp. 799–813, 2013.
- [5] R. J. Chokshi, H. Zia, H. K. Sandhu, N. H. Shah, and W. A. Malick, "Improving the dissolution rate of poorly water soluble drug by solid dispersion and solid solution-pros and cons," *Drug Delivery*, vol. 14, no. 1, pp. 33–45, 2007.
- [6] N.-Q. Shi, Y.-S. Lei, L.-M. Song, J. Yao, X.-B. Zhang, and X.-L. Wang, "Impact of amorphous and semicrystalline polymers on the dissolution and crystallization inhibition of pioglitazone solid dispersions," *Powder Technology*, vol. 247, pp. 211–221, 2013.
- [7] K. Jo, J. M. Cho, H. Lee et al., "Enhancement of aqueous solubility and dissolution of celecoxib through phosphatidylcholine-based dispersion systems solidified with adsorbent carriers," *Pharmaceutics*, vol. 11, no. 1, pp. 1–14, 2018.
- [8] S. Bialleck and H. Rein, "Preparation of starch-based pellets by hot-melt extrusion," *European Journal of Pharmaceutics and Biopharmaceutics*, vol. 79, no. 2, pp. 440–448, 2011.
- [9] J. O. Eloy and J. M. Marchetti, "Solid dispersions containing ursolic acid in Poloxamer 407 and PEG 6000: a comparative study of fusion and solvent methods," *Powder Technology*, vol. 253, pp. 98–106, 2014.
- [10] P. J. Marsac, T. Li, and L. S. Taylor, "Estimation of drug-polymer miscibility and solubility in amorphous solid dispersions using experimentally determined interaction parameters," *Pharmaceutical Research*, vol. 26, no. 1, pp. 139–151, 2009.
- [11] P. J. Marsac, S. L. Shamblin, and L. S. Taylor, "Theoretical and practical approaches for prediction of drug-polymer miscibility and solubility," *Pharmaceutical Research*, vol. 23, no. 10, pp. 2417–2426, 2006.
- [12] P. J. Marsac, H. Konno, A. C. F. Rumondor, and L. S. Taylor, "Recrystallization of nifedipine and felodipine from amorphous molecular level solid dispersions containing poly(vinylpyrrolidone) and sorbed water," *Pharmaceutical Research*, vol. 25, no. 3, pp. 647–656, 2008.
- [13] H. Chauhan, C. Hui-Gu, and E. Atef, "Correlating the behavior of polymers in solution as precipitation inhibitor to its amorphous stabilization ability in solid dispersions," *Journal of Pharmaceutical Sciences*, vol. 102, no. 6, pp. 1924–1935, 2013.
- [14] G. Zhao, Q. Zeng, S. Zhang et al., "Effect of carrier lipophilicity and preparation method on the properties of andrographolide-solid dispersion," *Pharmaceutics*, vol. 11, no. 2, pp. 74–91, 2019.
- [15] C. Calabrese, S. H. Berman, J. G. Babish et al., "A phase I trial of andrographolide in HIV positive patients and normal volunteers," *Phytotherapy Research*, vol. 14, no. 5, pp. 333–338, 2000.
- [16] P. K. Singha, S. Roy, and S. Dey, "Protective activity of andrographolide and arabinogalactan proteins from *Andrographis paniculata* nees. Against ethanol-induced toxicity in mice," *Journal of Ethnopharmacology*, vol. 111, no. 1, pp. 13–21, 2006.
- [17] N. Sermkaew, W. Ketjinda, P. Boonme, N. Phadoongsombut, and R. Wiwattanapatapee, "Liquid and solid self-microemulsifying drug delivery systems for improving the oral bioavailability of andrographolide from a crude extract of *Andrographis paniculata*," *European Journal of Pharmaceutical Sciences*, vol. 50, no. 3–4, pp. 459–466, 2013.
- [18] Y. Zhang, X. Hu, X. Liu et al., "Dry state microcrystals stabilized by an HPMC film to improve the bioavailability of

- andrographolide,” *International Journal of Pharmaceutics*, vol. 493, no. 1-2, pp. 214–223, 2015.
- [19] J. J. Sousa, A. Sousa, F. Podczec, and J. M. Newton, “Factors influencing the physical characteristics of pellets obtained by extrusion-spheronization,” *International Journal of Pharmaceutics*, vol. 232, no. 1-2, pp. 91–106, 2002.
- [20] G. Zhao, X. Liang, C. Wang, Z. Liao, Z. Xiong, and Z. Li, “Effect of superfine pulverization on physicochemical and medicinal properties of qili powder,” *Revista Brasileira de Farmacognosia*, vol. 24, no. 5, pp. 584–590, 2014.
- [21] E. Karavas, E. Georgarakis, M. P. Sigalas, K. Avgoustakis, and D. Bikiaris, “Investigation of the release mechanism of a sparingly water-soluble drug from solid dispersions in hydrophilic carriers based on physical state of drug, particle size distribution and drug-polymer interactions,” *European Journal of Pharmaceutics and Biopharmaceutics*, vol. 66, no. 3, pp. 334–347, 2007.
- [22] Y. Shibata, M. Fujii, M. Kokudai et al., “Effect of characteristics of compounds on maintenance of an amorphous state in solid dispersion with crospovidone,” *Journal of Pharmaceutical Sciences*, vol. 96, no. 6, pp. 1537–1547, 2007.
- [23] R. N. Shamma and M. Basha, “Soluplus®: a novel polymeric solubilizer for optimization of carvedilol solid dispersions: formulation design and effect of method of preparation,” *Powder Technology*, vol. 237, pp. 406–414, 2013.
- [24] G. Mohammadi, M. Barzegar-Jalali, H. Valizadeh et al., “Reciprocal powered time model for release kinetic analysis of ibuprofen solid dispersions in oleaster powder, microcrystalline cellulose and crospovidone,” *Journal of Pharmacy & Pharmaceutical Sciences*, vol. 13, no. 2, pp. 152–161, 2010.
- [25] L. Zhao, J. Ding, C. Xiao, X. Chen, G. Gai, and L. Wang, “Poly(L-glutamic acid) microsphere: preparation and application in oral drug controlled release,” *Acta Chimica Sinica*, vol. 73, no. 1, pp. 60–65, 2015.
- [26] P. Costa and J. M. Sousa Lobo, “Modeling and comparison of dissolution profiles,” *European Journal of Pharmaceutical Sciences*, vol. 13, no. 2, pp. 123–133, 2001.